

Ring Signature Index

Csaba L. Nagy, Mircea V. Diudea

Department of Chemistry, Faculty of Chemistry and Chemical Engineering,

Babes-Bolyai University, 400028 Cluj, Romania

diudea@chem.ubbcluj.ro

(Received February 11, 2016)

Abstract

Nanoworld is a term referring to the level of knowledge and transform of the matter, at the nanoscale level, both by nanoscience and nanotechnology. The nanoworld is “populated” by thousands of real 3D structures and millions of hypothetical constructions, of the rank 3 or higher. The need to distinguish among rather similar structures and prove their diversity is a challenging task that the present paper attempts to address. Topology was used as a theoretical tool for the design of a single number based on the ring signature, accounting for the configuration of rings around any vertex of a translational (or rotational) network. Mathematical properties, including the upper bound, of a new index, are exemplified on several structures, including the Platonic solids, some translational networks and some spongy hypercubes, of which substructures can be enumerated by combinatorial formulas accounting for the genus of the embedded surface, for the first time reported in literature.

1 Introduction

At the nanoscale, the world is “populated” with thousands of real 3D structures and millions of hypothetical constructions [1,2], of complexity (*i.e.*, rank [3,4]) 3 or higher. Among these, zeolites [5] define a class of (natural or synthetic) chemical compounds, of translational symmetry [6], consisting of voids, that may host ionic or neutral small specie, and channels that may work as molecular sieves, thus facilitating the matter exchange from the two parts of a porous wall [7–9]. Zeolites are spongy periodic networks [10–12], decorated with a variety of voids/shapes, starting with the basic Tetrahedron; even there are some few convex polyhedra [13–15] (triangular prism, hexagonal prism, gyrobisfastigium *i.e.*, J_{26} Johnson’s object [16], truncated octahedron and the cube) that can tessellate alone the 3D space, usually more than one type shape will achieve this task, that is the case of zeolites. Two basic descriptors are used to distinguish among the huge variety of networks [17–19]:

- (i) “Vertex symbol” (or “face symbol”), that describes the local topology of a vertex (more precisely, the faces/rings around any vertex) and
- (ii) “Tiling”, that gives the tiling signature (*i.e.*, shapes or voids around each tile) of a net.

A “tile” is a generalized polyhedron [18] that admits curved faces and vertices of degree 2 while a tiling is a filling of space by tiles sharing faces (*e.g.*, by face-to-face identification). Neither of these numbers provides a unique description of crystal structures.

The article is organized as follows: after the introductory part, the ring signature index RSI is defined in Sect. 2. The 3rd section provides a study on a translational network (and its medials) thus illustrating the utility of RSI in structure elucidation. Definition of spongy hypercubes and their combinatorial and RSI properties are given in Sect. 4. Conclusions and references will close the article.

2 Ring signature index

Define Ring Signature Index *RSI* as a collection of rings around the vertices of a network, as follows:

$$P(x)_i = \sum_s s \cdot x^{k_s} \quad (1)$$

$$RS_i = P'_i(1) / P_i(1) \quad (2)$$

$$RSI = (1 / qv) \sum_i RS_i \quad (3)$$

In the above, $P(x)_i$ is the polynomial of „ring occurrence” or the „ring signature”, or even the „vertex configuration”, with s being the size of a „strong” ring occurring k_s -times around each point i . Next, RS_i calculates a „mean ring signature” as the ratio (in $x=1$) of the first derivative to the „zero” derivative of the ring occurrence polynomial. Finally, (eq 3), the summation of RS_i , which runs over all vertices “ v ” in the whole molecule (or a “domain” of a translational structure), is again mediated “per vertex” and per vertex orbits “ q ” (under the full symmetry group) existing in the whole considered structure. Here „strong” denotes a ring that is not the sum of other smaller rings [18]. However, the ring notion may be extended to „circuit” notion, in getting more comprehensive information about the topology of the network.

Proposition 1. At the same occurrence k , the mean ring signature RS_i is an integer number, irrespective of the ring size.

The proof comes from the RS_i definition, as follows: denote by k_{s1} and k_{s2} the (integer number) occurrence of two rings around a vertex, of size s_1 and s_2 ; since $k_{s1} = k_{s2} = k$ (same occurrence), then:

$$RS_i = (s_1 \cdot k_{s_1} + s_2 \cdot k_{s_2}) / (s_1 + s_2) = k(s_1 + s_2) / (s_1 + s_2) = k \quad (4)$$

Proposition 2. Isohedral graphs show integer RS_i since they have a single ring type (*i.e.*, are face transitive) and a single occurrence number:

$$RS_i = sk / s = k \quad (5)$$

Proposition 3. There exist graphs that show different occurrence for the same ring size; in such a case, RS_i may be non-integer, according to the parity of occurrence numbers sum:

$$RS_i = (s \cdot k_1 + s \cdot k_2) / 2s = s(k_1 + k_2) / 2s = (k_1 + k_2) / 2 \quad (6)$$

The above statements were formulated for isohedral (and isogonal, *i.e.* vertex transitive) graphs, where $q=1$ and $RS_i = RSI$. However, isohedral graphs are not always isogonal: the Catalan solid graphs (which are duals to Archimedean) are all face-transitive but not vertex-transitive. In vertex non-transitive structures, $q > 1$ and the global index RSI may be a non-integer number, according to the numbers parity.

Theorem. *The upper bound of ring signature index RSI can be combinatorially calculated from the vertex degree by $\binom{Deg}{2}$; this is reached in isohedral and isogonal graphs with no self-intersection of strong rings.*

Demonstration comes from the above propositions, basically from proposition 2. It is well-known that the maximum number of rings around a vertex equals the combination of the number of its connections (*i.e.*, degrees, Deg) [20,21] taken two. This is the case described by eq. (5): $RS_{i,max} = k_{max} = \binom{Deg}{2}$. However, some isohedral graphs can be seen as “networks” (*i.e.*, with rings that intersect to each other), like Icosahedron I, Octahedron O, 16-Cell, 24-Cell, etc.; in such cases, the set of connections is split, at least in two subsets (for which, *e.g.*, $Deg = Deg_1 + Deg_2$) and, because $\binom{Deg}{2} > \binom{Deg_1}{2} + \binom{Deg_2}{2}$, the maximum value of RS_i is less than k_{max} (see Table 1, *e.g.*, 24-Cell_net). The case $Deg_1 = Deg_2$ recovers the case of eq (4), with $RS_i = k < k_{max}$. Since the isogonal graphs have only one vertex orbit ($q=1$), it means that $RS_i = RSI$ and the theorem is demonstrated. Maximal RSI values are found in Dodecahedron D, Tetrahedron T or the Hypercube Q_n .

The case of relation (6) is found in the “spongy-hypercube” (see Section 4): since here $k_1 + k_2 = k_{max}$, then $RS_i = \text{Combin}(Deg, 2) / 2$, in words, RS_i equals the half of the upper bound value. Data in Table 1 and in the following ones support the above theorem.

Table 1. Ring signature index RSI in some cells and nets.

Structure	v	v_i	q	Deg	Ring signature	RSI	$\left(\begin{matrix} Deg \\ 2 \end{matrix}\right)$
D	20	20	1	3	5^3	3	3
I	12	12	1	5	3^5	5	10
C	8	8	1	3	4^3	3	3
O	6	6	1	4	3^4	4	6
T	4	4	1	3	3^3	3	3
I_net	12	12	1	5	$3^5.5^5$	5	10
O_net	6	6	1	4	$3^4.4^2$	2.857	6
16-Cell	8	8	1	6	3^{12}	12	15
16-Cell_net	8	8	1	6	$3^{12}.4^3$	6.857	15
24-Cell	24	24	1	8	3^{12}	12	28
24_Cell_net	24	24	1	8	$3^{12}.4^{12}$	12	28
C ₆₀	60	60	1	3	$5^1.6^2$	1.546	3

3 Ring signature in a translational network

Structure elucidation in Chemistry in general, and particularly in Crystallography, makes appeal of instrumental techniques but also of theoretical tools. In this respect, RSI would be of real interest in classification of networks, both radial and translational and in an accurate description of complex molecular/ionic structures.

The network focused on hereafter was built starting from the Octahedron by stellation *st*, followed by truncation *t*, operations resulted in the cluster C72A= 24@TT.222.72, of which shapes are detailed as TO@(8TT;6HCO).72 (see Figure 1). (For map operations, the reader is invited to consult refs. [22–27]. The name of clusters is written in a “shell-by-shell” manner [28,29], starting with the core (symbolized either by the shortened names of the consisting shape: TT = truncated Tetrahedron; TO = truncated Octahedron; CO = Cuboctahedron, or by the number of atoms of that shape) endohedrally @ included into the next (outer) shell(s), while is suffixed by the number of atoms in the whole structure. The net is made by self-assembly of TT (by “face-to-face” gluing/ identification), which is reflected in the name we give to this net: C72@TT, delimited as a cubic domain, e.g., C72@TT.222.72, where “222” means 2×TT along the directions of translation; the name is suffixed by the global number of points/atoms in the considered domain. According to the map operations that provided this network, it is named as *t(st(O))72@TT*. The letter “A” in the name specifies the “net” while “B” denotes the “co-net”, net/co-net being interchangeable; the letter “H” in the front of shape symbols means “half”, used to avoid fractional numbers in the name of clusters.

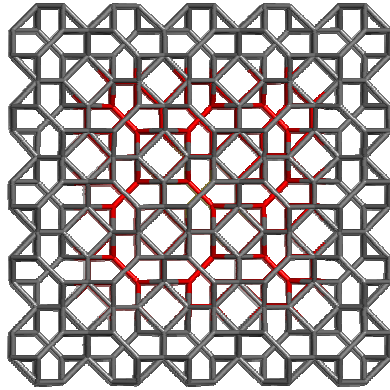
The network $C72@TT$ (synonyms: UB12, sqc7309, 5/3/c4; Tiling: 2TT+CO+TO; Space Group: $Fm\bar{3}m$ [30]; uninodal, of degree 5, with the topology (ring signature): $3^2.4^2.6^6$; the value of RSI corresponding to this vertex symbol is 3.846 (Table 2), that reflects its high topological symmetry (e.g., a single vertex/atom equivalence class – see also refs. [31,32]). The ring signature was obtained by selecting the $C72@TT.333.216$ (that contains the three shapes of the net: TT, TO and CO) within a larger domain, e.g., $C216@TT.555.900$. The ref. [30] assumes E2 for the two classes of edges and no specification about the faces/rings classes.

To verify this result, we applied to $C72@TT$ the “medial” m operation [33] (also known as “rectification” or “ambo” [34]) thus resulting the net $m(C72)132@mTT$ (Figure 2, left). A “spongy” version $m(C72)132X@mTTX$ (Figure 2, right) was obtained by the “Open” Op map operation applied to the initial medial. The both nets show two classes of vertices, corresponding to the parent edges.

Next, the face-dual operation applied to $C72@TT$ resulted in $d(C72)70@dTT$ net (Figure 3). This new net consists in three classes of vertices with the population: {36}; {108} and {108}, in the selection $dC216.252@dTT.555.1240$, as were the faces in the parent cluster $C216$ (squares, triangles and hexagons, respectively).

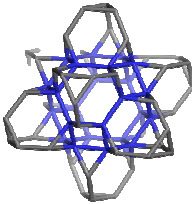
Table 2. Ring signature index RSI in $C72A=24@TT.222.72$ and $C72B=12@TT.222.72$ clusters

	Structure	v	v_i	q	Deg	Ring signature	RSI
1	$TO_{sel}@TT.444.480$	24	24	1	5	$3^2.4^2.6^6$	3.846
2	$C72A_{sel}@TT.444.480$	72	72	1	5	$3^2.4^2.6^6$	3.846
3	C72A	72	24	2	5	$3^2.4.6^4$	0.992
			48		3	3.6^2	
			24		5	$3^2.6^4$	
4	$C72A@TT.480$	480	168	4	5	$3^2.4^2.6^6$	0.676
			96		5	$3^2.4.6^4$	
			192		3	3.6^2	
5	$CO_{sel}@TT.444.480$	12	12	1	5	$3^2.4^2.6^6$	3.846
6	$C72B_{sel}@TT.444.480$	72	72	1	5	$3^2.4^2.6^6$	3.846
			12		5	$3^2.6^4$	
			12		5	$3^2.4^2.6^6$	
7	C72B	72	12	3	5	$3^2.4^2.6^6$	0.769
			48		3	3.6^2	
			12		5	$3^2.6^4$	
8	$C72B@TT.480$	480	156	4	5	$3^2.4^2.6^6$	0.664
			120		5	$3^2.4.6^4$	
			192		3	3.6^2	

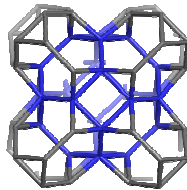


C216@TT.555.900

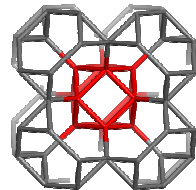
1. $3^2.4^2.6^6$; | {216} | deg = 5 ; RSI=3.84615 (uninodal)
(Selection 216/900)



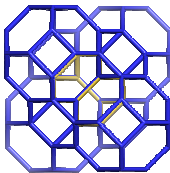
24@8TT.72
t(st(O)).72



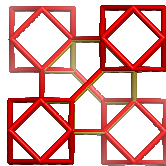
C72A=24@TT.222.72
TO@(8TT+6HCO).72



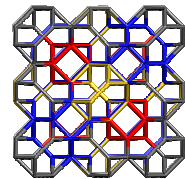
C72B=12@TT.222.72
CO@(8TT+6HTO).72



TT@4TO.84



TT@4CO.48



C216=C72@TT.333.216
TT@(4TO+4CO+6TT)@(8TT+
12TT).216

Figure 1. Network C72@TT with a selection C216@TT.555.900 and its substructures (bottom). Its three shapes are: TT (truncated Tetrahedron)=[$3^4.6^4$]; TO (truncated Octahedron)=[$4^6.6^8$] and CO (Cuboctahedron)= [$3^8.4^6$]; “H” means “half”. Tiling signature: TT@(4TO+4CO+6TT); TO@(6CO+8TT); CO@(6TO+8TT).

Figure count (see Sect. 4) in the clusters C216 and C432 (and their substructures) confirmed their assigned structures and the rank 4 (Tables 3 and 4). Interestingly, the cluster C432X accounts for the rank 5, being bound by its 8 subunits of rank 4 (Table 5). We found a similar behavior in spongy hypercubes [35]. The trend of RSI is far from being completely understood; in this respect more examples are needed.

Table 3. Figure count in C216 and its relatives.

Structure	v	e	3(2)	4(2)	6(2)	2	3	χ	Rank
C216	216	432	108	36	108	252	36	0	4
C72A	72	132	32	6	32	70	10	0	4
C72B	72	132	32	6	32	70	10	0	4

Table 4. Figure count in $mC216=C432$ and its relatives.

Structure	v	e	3(2)	4(2)	6(2)	2	3	χ	Rank
$mC216$	432	1188	648	144	108	900	144	0	4
C132A	132	336	176	30	32	238	34	0	4
C132B	132	336	176	30	32	238	34	0	4

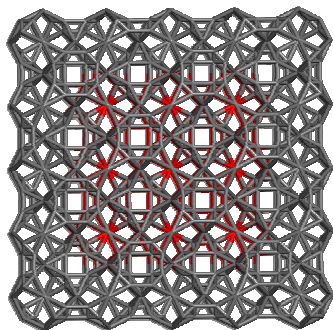
Table 5. Figure count in $mC216X$ and its spongy relatives.

Structure	v	e	3(2)	6(2)	2	3	4	χ	g	Rank
$mC216X$	432	972	432	108	540	28	8	-20	11	5
C132A	132	288	128	32	160	8	0	-4	3	4
C132B	132	288	128	32	160	8	0	-4	3	4

4 Spongy structures of higher rank

Generalization of a polyhedron to n -dimensions is called a polytope [36–38]. The n -dimensional spaces (in the geometrical sense) may be avoided if one refers to abstract polytopes [39]; properties like angles, edge lengths, etc. are disregarded (as in the Graph Theory) and only the combinatorial properties of structures are considered. The notion of “dimension” is substituted with that of “rank” [3,4,40]. No space, such as Euclidean space, is required to contain an abstract polytope; its combinatorial properties may be expressed as a partially ordered set or a poset [3,4,41].

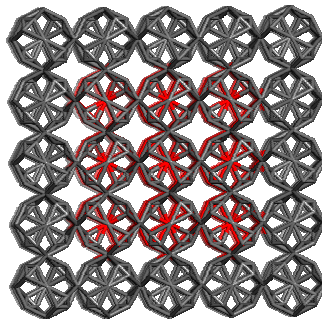
In an abstract n -polytope the “vertex figure” at a given vertex is an $(n-1)$ -polytope. In polyhedra the vertex figure can be represented by the “vertex configuration” which lists “sequence of faces” around that vertex. In crystallography this is called the “face symbol” [18].



C432@mTT.555.1950

mC216.432@mTT.555.1950

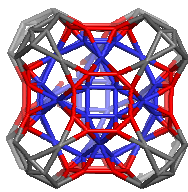
1. $3^8.6^4$; $\{108\}$ | deg = 8 |
 2. $3^5.4^3.6$; $\{324\}$ | deg = 6 |
- RSI=1.61859 (Sel. 432/1950)



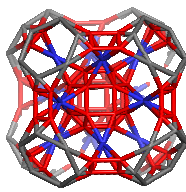
C432X@mTTX.555.1950

mC216.432X@mTTX.555.1950

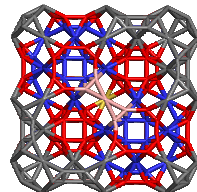
1. $3^4.6^4$; $\{108\}$ | deg = 8 |
 2. $3^3.6$; $\{324\}$ | deg = 4 |
- RSI=1.12500 (Sel. 432/1950)



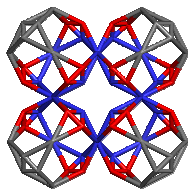
C132A=mtO@mtT.222.132



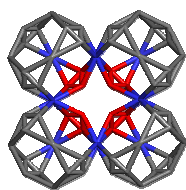
C132B=mmC@mtT.222.132



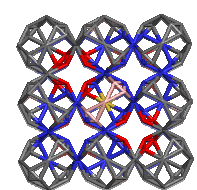
C432
m(C72)132@mTT.333.432



C132XA (C4)
Op(mTO)@mTT.222.132



C132XB (C4)
Op(mCO)@mTT.222.132

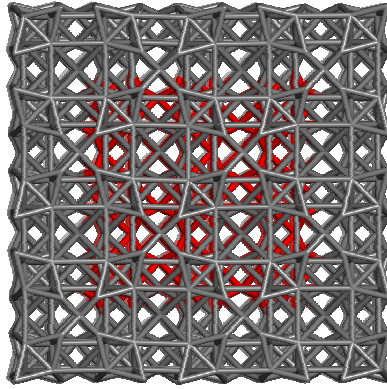


C432X (C2)
m(C72)132X@mTTX.333.432

Tiling signature:

- (filled) *mtT@(4mtO+4mmC+6mtT)*; *mtO@(6mmC+8mtT)*; *mmC@(6mtO+8mtT)*
 (spongy) *mtT@(4Op(mtO)+4Op(mmC)+6mtT)*; *Op(mtO)@(6Op(mmC)+8mtT)*;
Op(mmC)@(6Op(mtO)+8mtT)

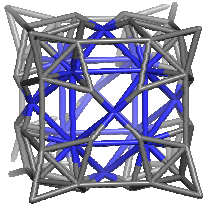
Figure 2. Medial derivatized nets *m(C72)132@mTT* of the parent *C72@TT* net, with their selections *C432X@mTTT.555.1950* ($X=Op$, for the spongy medial net) and their substructures (bottom).



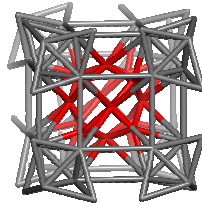
dC216.252@ dTT.555.1240

1. $3^8 \cdot 4^4$; $|\{36\}$ (squares) | deg = 8 |
2. $3^6 \cdot 4^3$; $|\{108\}$ (triangles) | deg = 6 |
3. $3^8 \cdot 18 \cdot 4^6$; $|\{108\}$ (hexagons) | deg = 12 |

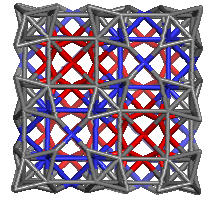
RSI=2.47619 (Selection 252/1240)



C70A
dC72A=dTO@dTT.222.70



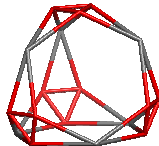
C70B
dC72B=dCO@dTT.222.70



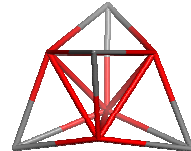
C252
dC216.252=dTT.333.252



TT.12
 $[12(3 \cdot 6^2)]$



*m*TT.18
 $[12(3^3 \cdot 6) + 6(3^2 \cdot 6^2)]$



*d*TT.8 = *st*T.8
 $[4(3^3) + 4(3^9)]$

Figure 3. Network *d(C72)70@dTT* with a selection *C252@dTT.555.1240* and its substructures (bottom).

The alternating sum [42,43] of k -faces contained in an n -ranked polytope gives 2 and zero for n odd and even, respectively.

$$\sum_{k=0}^{n-1} (-1)^k f_k = 1 - (-1)^n \tag{7}$$

For polyhedra (of rank 3) on orientable surfaces of genus g , one obtains the classical Euler (1758) relation (8) [42]:

$$v - e + f = \chi = 2(1 - g) \tag{8}$$

The Euler characteristic χ , calculated by (8), is a dimensionless quantity associated with an object; it is, in fact, a generalization of the cardinality [44]. Positive/negative χ values indicate positive /negative curvature of a polyhedral structure [25]. Genus g is the number of tori contained in an orientable surface on which the polyhedral graph is embedded [20].

Hypercube Q_n is an n -dimensional analogue of the Cube ($n=3$), also called an n -cube. It is a regular graph of degree n , according to Balinsky's theorem [45]. The graph of Hypercube may be drawn by the Cartesian product of n edges: $(P_2)^{\square n} = Q_n$. The n -cube is written by the Schläfli symbols [43] as $\{4, 3^{n-2}\}$; the number of k -faces contained in an n -cube $Q_n(k)$ comes from the coefficients of $(2k+1)^n$ in the binomial expansion.

$$Q_n(k) = 2^{n-k} \binom{n}{k}; \quad k = 0, \dots, n - 1 \tag{9}$$

Hypercube may be embedded in surfaces other than the sphere [35].

Let now take a polyhedral graph $G(v)$ of a 3-connected polyhedron on v -vertices and make n -times the Cartesian product with an edge; the operation results in a "spongy hypercube" $G(v, Q_n) = G(v) \square^n P_2$. On each edge of the original polyhedral graph, a local hypercube Q_n will evolve; it means that, in a spongy hypercube, the original 2-faces will not be counted. Figure 4 illustrates such spongy hypercubes, embedded in the Cube and Dodecahedron, respectively.

Conjecture. *The k -faces of a spongy hypercube $G(v, Q_n)$, built on a 3-connected polyhedron of v -vertices, are combinatorially counted from the previous rank faces; their alternating summation accounts for the genus of the surface where Hypercube Q_n is embedded [33].*

$$G(v, Q_n, k) = (v/n) [3n - 2(n - k)] \cdot 2^{(n-k-1)} \cdot \binom{n}{k}; \quad n > 1; k = 0, 1, \dots, n \tag{10}$$

$$\sum_{k=0}^n (-1)^k f_k = \chi(M) = 2(1 - g); \quad n > 1; k = 0, 1, \dots, n \tag{11}$$

Formula (10) represents the “embedding” of the hypercube on any 3-connected polyhedral graph (see the factor in the front of the almost classical hypercube counting (9)), that transforms the embedding polyhedron in a multi-toroidal hypercube [33]. More precisely, the “spongy hypercube” is the union of the original polyhedron and the hypercubes developed on each edge of the parent polyhedral graph $G(v)$.

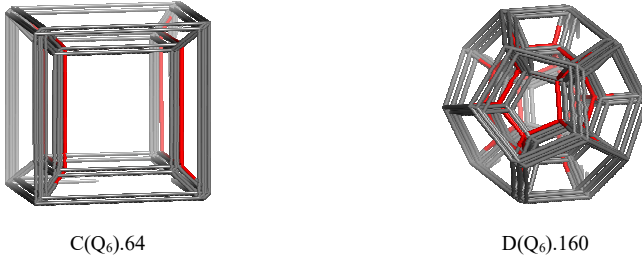


Figure 4. Spongy hypercubes: cubic $C(Q_6)$ (top, left); dodecahedral $D(Q_6)$ (top right) and their parents (bottom)

Table 6. Ring signature index RSI in Hypercube Q_n and its spongy view $C(Q_n)$.

v	Deg	n	Q_n			$C(Q_n)$		
			Ring signature	RSI	$\binom{Deg}{2}$	Ring signature	RSI	$\binom{Deg}{2}$
8	3	3	4^3	3	3	4^3	3	3
16	4	4	4^6	6	6	$4^3.4^3$	3	6
32	5	5	4^{10}	10	10	$4^7.4^3$	5	10
64	6	6	4^{15}	15	15	$4^{12}.4^3$	7.5	15
128	7	7	4^{21}	21	21	$4^{18}.4^3$	10.5	21
256	8	8	4^{28}	28	28	$4^{25}.4^3$	14	28

Table 7. Ring signature RSI in Dodecahedral and Tetrahedral spongy hypercube $D(Q_n)$.

Structure	v	Deg	Ring signature	RSI	$\binom{Deg}{2}$
$D(Q_n)$	20	3	5^3	3	3
	40	4	$4^3.5^3$	3	6
	80	5	$4^7.5^3$	4.77778	10
	160	6	$4^{12}.5^3$	7	15
	320	7	$4^{18}.5^3$	9.66666	21
$T(Q_n)$	4	3	3^3	3	3
	8	4	$3^3.4^3$	3	6
	16	5	$3^3.4^7$	5.28571	10
	32	6	$3^3.4^{12}$	8.14286	15
	64	7	$3^3.4^{18}$	11.57143	21

Compare the formula (11) with the previous formulas (7) and (8): it expresses the “spongy” character [28] of these structures by the genus [20] g of the hypersurface. Genus also means the number of connections of a surface; it equals, as Diudea conjectured in [33], the half sum of “window”- faces f_w , coming from the parent polyhedron: $g=f_w(G(v))/2$. Note that (11) ignores the (hyper-) prisms evolving on each parent face of the original polyhedron [33]. However, counting the substructures of “spongy” hypercubes precisely follows the combinatorial rules and the presence of “genus” in (11) represents the *essence* of this novel approach, not yet described in the literature, excepting the case $n=3$. In this respect, the case of full-hypercube is compared with the case of spongy-hypercube in the calculus of ring signature index (Table 6). For the dodecahedral and tetrahedral spongy hypercube, as rotational networks, the values of this index are given in Table 7.

5 Conclusions

Topology of nanostructures, both of translational and rotational networks, may be described by the newly proposed Ring Signature Index *RSI*, as was herein illustrated. The index shows the upper bound in highly symmetric isohedral structures and in hypercubes of rank 3 and higher. *RSI* is a promising tool in the quick exploring and classification of databases, by the inclusion of topological equivalence classes. Further studies will provide more evidence of *RSI* properties and usefulness. Spongy hypercubes were used for the evaluation of discriminating ability of *RSI*. Their substructure counting was achieved by combinatorial formulas, reported here for the first time in the literature.

Acknowledgement: The authors greatly acknowledge the financial support offered by Romanian UEFISCDI grant no.PN-II-ID-PCE-2011-3-0346.

References

1. M. V. Diudea, C. L. Nagy (Eds.), *Diamond and Related Nanostructures*, Springer, Dordrecht, 2013.
2. V. Y. Shevchenko, *Search in Chemistry, Biology and Physics of the Nanostate*, Lema, St. Petersburg, 2011.
3. E. Schulte, Regular incidence-polytopes with Euclidean or toroidal faces and vertex-figures, *J. Comb. Theory A* **40** (1985) 305–330.
4. E. Schulte, Polyhedra, complexes, nets and symmetry, *Acta Cryst. A* **70** (2014) 203–216.
5. W. M. Meier, D. H. Olson, *Atlas of Zeolite Structure Types*, Butterworth-Heineman, London, 1992.

6. M. Hargittai, I. Hargittai, *Symmetry Through the Eyes of a Chemist*, Springer, Dordrecht, 2010.
7. X. Blasé, G. Benedek, M. Bernasconi, Structural, mechanical, and superconducting properties of clathrates, in: L. Colombo, A. Fasolino (Eds.), *Computer-Based Modeling of Novel Carbon Systems and Their Properties*, Springer, Dordrecht, 2010, pp. 171–206.
8. A. J. Karttunen, T. F. Fässler, M. Linnolahti, T. A. Pakkanen, Structural principles of semiconducting group 14 clathrate frameworks, *Inorg. Chem.* **50** (2011) 1733–1742.
9. U. Schwarz, A. Wosylus, B. Böhme, M. Baitinger, M. Hanfland, Y. Grin, A 3D network of four-bonded germanium: a link between open and dense, *Angew. Chem. Int. Ed.* **47** (2008) 6790–6793.
10. V. A. Blatov, O. Delgado-Friedrichs, M. O’Keeffe, D. M. Proserpio, Three-periodic nets and tilings: natural tilings for nets, *Acta Crystall.* **A 63** (2007) 418–425.
11. I. A. Baburin, D. M. Proserpio, V. A. Saleev, A. V. Shipilova, From zeolite nets to sp³ carbon allotropes: a topology-based multiscale theoretical study, *Phys. Chem. Chem. Phys.* **17** (2015) 1332–1338.
12. N. A. Anurova, V. A. Blatov, G. D. Ilyushin, D. M. Proserpio, Natural tilings for zeolite-type frameworks, *J. Phys. Chem. C* **114** (2010) 10160–10170.
13. H. S. M. Coxeter, *Regular Polytopes*, Dover, New York, 1973.
14. B. Grünbaum, *Convex Polytopes*, Wiley, New York, 1967.
15. B. Grünbaum, G. S. Shephard, *Tillings and Patterns*, Freeman, New York, 1987.
16. N. W. Johnson, Convex polyhedra with regular faces, *Can. J. Math.* **18** (1966) 169–200.
17. O. Delgado-Friedrichs, M. O’Keeffe, Crystal nets as graphs: terminology and definitions, *J. Solid State Chem.* **178** (2005) 2480–2485.
18. V. A. Blatov, M. O’Keeffe, D. M. Proserpio, Vertex-, face-, point-, Schläfli-, and Delaney-symbols in nets, polyhedra and tilings: recommended terminology, *Cryst. Eng. Comm.* **12** (2010) 44–48.
19. V. A. Blatov, Multipurpose crystallochemical analysis with the program package TOPOS, *IUCr Comp. Comm. Newsletter* **7** (2006) 4–38.
20. F. Harary, *Graph Theory*, Addison–Wesley, Reading, 1969.
21. M.V. Diudea, I. Gutman, L. Jäntschi, *Molecular Topology*, Nova, New York, 2002.
22. T. Pisanski, M. Randić, Geometry at work, *MAA Notes*, **53** (2000) 174–194.
23. M. V. Diudea, M. Ştefu, P. E. John, A. Graovac, Generalized operations on maps, *Croat. Chem. Acta* **79** (2006) 355–362.
24. V. Eberhard, *Zur Morphologie der Polyeder*, Teubner, Leipzig, 1891.
25. M. V. Diudea, C. L. Nagy, *Periodic Nanostructures*, Springer, Dordrecht, 2007.
26. M. V. Diudea, *Nanomolecules and Nanostructures – Polynomials and Indices*, Univ. Kragujevac, Kragujevac, 2010.
27. M. V. Diudea, Nanoporous carbon allotropes by septupling map operations, *J. Chem. Inf. Model.* **45** (2005) 1002–1009.
28. M. V. Diudea, Quasicrystals: between spongy and full space filling, in: M. V. Diudea, C. L. Nagy (Eds.), *Diamond and Related Nanostructures*, Springer, Dordrecht, 2013, pp. 335–385.

29. M. V. Diudea, A. Bende, C. L. Nagy, Carbon multi-shell cages, *Phys. Chem. Chem. Phys.* **16** (2014) 5260–5269.
30. <http://rcsr.net/nets/ubt>.
31. M. V. Diudea, V. R. Bucila, D. M. Proserpio, 1-periodic nanostructures, *MATCH Commun. Math. Comput. Chem.* **70** (2013) 545–564.
32. M. Ştefănuţ, A. Parvan-Moldovan, F. Kooperazan-Moftakhar, M. V. Diudea, Topological symmetry of C_{60} -related multi-shell clusters, *MATCH Commun. Math. Comput. Chem.* **74** (2015) 273–284.
33. E. Steinitz, *Polyeder und Raumeinteilungen*, *Encyclopädie der Mathematischen Wissenschaften*, Band 3 (Geometries), 1922, pp. 1–139.
34. J. H. Conway, H. Burgiel, C. Goodman-Strass, *The Symmetries of Things*, Peters, Wellesley, 2008.
35. M. V. Diudea, *Multi-Shell Polyhedral Clusters*, Springer, 2016 (in preparation).
36. B. Grünbaum, G. C. Shephard, *Tilings and Patterns*, Freeman, New York, 1987.
37. B. Grünbaum, *Convex Polytopes*, Springer, New York, 2003.
38. H. S. M. Coxeter, *Regular Complex Polytopes*, Cambridge Univ. Press, Cambridge, 1974.
39. E. Schulte, *Regular Incidence Complexes*, PhD thesis, Dortmund Univ., 1980.
40. E. Schulte, Symmetry of polytopes and polyhedral, in: J. E. Goodman, J. O'Rourke, *Handbook of Discrete and Computational Geometry*, Chapman & Hall/CRC Press, Boca Raton, 2004, pp. 311–330.
41. P. McMullen, E. Schulte, *Abstract Regular Polytopes*, Cambridge Univ. Press, Cambridge, 2002.
42. L. Euler, Elementa doctrinae solidorum, *Novi Comm. Acad. Scient. Imp. Petrop.* **4** (1758) 109–160.
43. L. Schläfli, *Theorie der Vielfachen Continuität Zürcher und Furrer*, Zürich, 1901 (Reprinted in: Ludwig Schläfli, 1814–1895, *Gesammelte Mathematische Abhandlungen*, Band 1, 167–387, Verlag Birkhäuser, Basel, 1950).
44. T. Leinster, The Euler characteristic of a category, *Doc. Math.* **13** (2008) 21–49.
45. M. L. Balinski, On the graph structure of convex polyhedra in n -space, *Pacific J. Math.* **11** (1961) 431–434.